Proc. Natl. Acad. Sci. USA
Vol. 88, pp. 11559–11563, December 1991
Neurobiology

High-resolution optical imaging of functional brain architecture in the awake monkey

(behaving monkey/ocular dominance/striate cortex/vision/cytochrome oxidase blobs)

AMIRAM GRINVALD*†‡, RON D. FROSTIG*§, RALPH M. SIEGEL*, AND EYAL BARTFELD*‡

*Laboratory of Neurobiology, The Rockefeller University, New York, NY 10021; †IBM Research Division, Yorktown Heights, NY 10598; and ‡The Weizmann Institute of Science, Rehovot, Israel

Communicated by James L. McGaugh, September 16, 1991 (received for review June 21, 1991)

ABSTRACT **Optical imaging of the functional architecture of cortex, based on intrinsic signals, is a useful tool for the study of the development, organization, and function of the living mammalian brain. This relatively noninvasive technique is based on small activity-dependent changes of the optical properties of cortex. Thus far, functional imaging has been performed only on anesthetized animals. Here we establish that this technique is also suitable for exploring the brain of awake behaving primates. We designed a chronic sealed chamber and mounted it on the skull of a cynomolgus monkey (*Macaca fascicularis*) over the primary visual cortex to permit imaging through a transparent glass window. Restriction of head position alone was sufficient to eliminate movement noise in awake monkey imaging experiments. High-resolution imaging of the ocular dominance columns and the cytochrome oxidase blobs was achieved simply by taking pictures of the exposed cortex when the awake monkey was viewing video movies alternatively with each eye. Furthermore, the functional maps could be obtained without synchronization of the data acquisition to the animal's respiration and the electrocardiogram. The wavelength dependency and time course of the intrinsic signal were similar in anesthetized and awake monkeys, indicating that the signal sources were the same. We therefore conclude that optical imaging is well suited for exploring functional organization related to higher cognitive brain functions of the primate as well as providing a diagnostic tool for delineating functional cortical borders and assessing proper functions of human patients during neurosurgery.**

The awake monkey preparation has offered many advantages for the study of higher cognitive functions (1). First, there are many questions that cannot be investigated by using anesthetized animals, simply because the brain of the anesthetized animal cannot perform the same remarkable computational tasks that the awake brain performs, especially in cortical regions other than primary sensory areas (2–6). Second, by manipulating the animal's behavior, it has been possible to begin to answer questions about the neuronal basis of higher cognitive functions. For example, how does the response of the neurons depend on behavioral states of the animal such as attention and motivation (7–10)? Finally, long-term physiological studies are possible in awake primates, allowing the investigation of development (11) and plasticity of the brain (12, 13).

Single unit recordings have been used for most of the recent explorations in the awake monkey preparation (12–16). This powerful technique is limited, however, to the measurement of the activity of very few neurons at a time. Local field potential measurement of brain activity has been made (17–19); however, its resolution is inadequate for high-resolution functional mapping of cortex. Furthermore, the interpretation of the results may be difficult due to the nonisotropic electrical properties of cortical tissue.

Two optical methods currently can provide information that is hard to obtain with electrical recording from the mammalian cortex *in vivo*. Optical imaging based on intrinsic signals (20) is useful for mapping the functional architecture of cortex and for studying neuronal interaction at adjacent cortical sites. Real-time optical imaging based on suitable voltage-sensitive dyes (21, 22) offers the imaging of population activity (rather than single cells) with millisecond time resolution. However, these two techniques have to date been used only in anesthetized animals.

Our goal was to investigate whether *in vivo* optical imaging in the awake behaving monkey is feasible. Was it actually possible to obtain high-resolution functional maps? To test this, we decided to image the ocular dominance columns (23) and cytochrome oxidase blobs (24–26). Difficulties were expected because in the anesthetized animal experiments it is necessary to use a subtraction procedure to remove the relatively large optical noise produced by the cardiac pulsations and respiratory movements to image the very small activity-dependent signals. First we examined whether this noise reduction approach was essential to obtaining reasonable optical signals and whether elimination of noise resulting from body motion of the alert monkey was possible. Second, since thus far positron emission tomography (PET) studies failed in anesthetized subjects (27), and since the optical imaging is based on signals largely originating from the microcirculation (28), we investigated whether the anesthetic or the paralytic drugs had an effect on the intrinsic signals to be optically imaged. The present work describes the successful application of optical imaging of neural activity based on intrinsic signals in the awake monkey. The resolution of these questions suggests that combined optical imaging and cognitive studies in human and nonhuman primate subjects are possible.

MATERIALS AND METHODS

Animals. The study was performed on a 3-year-old female cynomolgus monkey (*Macaca fascicularis*; 3 kg). The monkey was trained to sit quietly in a Plexiglas primate chair and view a video monitor. Juice was given as reinforcement. After this elementary training, the first surgical procedure to prepare the animal for optical recording was performed. Two anesthetized cynomolgus monkeys were also used for comparative study (Pentothal anesthesia; see refs. 28 and 29 for standard methods).

Surgical Procedures. General anesthesia of 1% isoflurane with 3:2 ratio of NO_2/O_2 and completely aseptic conditions were used. Titanium screws (Synthes, Paolo, PA) were implanted in the skull; a dental acrylic cap was built over

The publication costs of this article were defrayed in part by page charge payment. This article must therefore be hereby marked "*advertisement*" in accordance with 18 U.S.C. §1734 solely to indicate this fact.

Abbreviations: PET, positron emission tomography; EKG, electrocardiogram.

§Present address: Department of Psychobiology, University of California, Irvine, CA 92717.

them. The flat base of a 4-cm-long stainless steel bar was implanted in the dental acrylic for attachment of the monkey's head to the heavily reinforced, vibration-free monkey chair. Appropriate analgesics and antibiotics were given postoperatively.

Optical Chambers. Two optical chambers were mounted above the primary visual cortex in each hemisphere. The chambers had two critical differences from those developed for optical imaging in anesthetized animals. First, to protect the transparent cover glass a protective stainless steel cover could be threaded on top of the chamber. Second, the two long stainless steel tubes previously used for replacement of the artificial cerebrospinal fluid in the chamber were replaced by an indented inlet and outlet that could be blocked by stainless screw caps. The new chamber was a 20-mm-diameter cylinder, with soldered inlet and outlet attachments (diameter 3 mm, height 8 mm) at the two opposite sides of the chamber. To seal the chamber, a silicone rubber O-ring was used; the transparent glass or Plexiglas cover was put over the O-ring and pressed against it with a threaded stainless steel ring (width 1.3 mm). The stainless steel ring was 2.5 mm high and was internally threaded. The protective stainless steel cover was threaded onto this ring whenever the monkey was not in the recording chair. Dental acrylic surrounded the chambers from all sides flush with the upper surface of the chamber.

Experimental Preparations. After a 2-week recovery period, the monkey was trained to sit quietly in the chair with her head held in a fixed position and to ignore the shutters opening and closing in front of each eye. To minimize vibrations during the optical measurement, several thick bars solidly held the monkey chair to a heavy table (Newport, Fountain Valley, CA). A drop of juice was given as a reward for sitting quietly after three presentations. A few days prior to recording, the chamber was opened, under general anesthesia and sterile conditions, and the skull at the center of the chamber was removed with a 12 mm trephine. The chamber was rinsed with saline, filled with standard artificial cerebrospinal fluid, and then sealed.

Optical Imaging. The optical images of the cortical activity were collected by using a charge-coupled device camera (28, 29). For a daily recording session, the monkey was placed in the chair, her head was fixed, and the outer steel cover of the chamber was removed to reveal the transparent chamber window. The camera was then placed over the chamber and an image of the cortex was taken. To emphasize the vascular pattern, the cortex was illuminated with green light (540 nm) via light guides. The camera was then focused to image a region of cortex. Interference filters were used to select the proper wavelength for imaging the functional architecture, usually 630 nm (bandwidth 30 nm). In previous imaging experiments on anesthetized animals, the wavelength range of 600–630 nm provided the best signal-to-noise ratio.

Visual Stimulus. An IBM/AT computer equipped with a Sergeant Pepper (Number Nine, Cambridge, MA) video board served as a general-purpose visual stimulator. The stimuli in this study consisted of either drifting oriented bars or gratings displayed on a Sony Multisync monitor at 60 Hz. We also used more natural stimuli; a video movie, *Winnie the Pooh*, was presented to the monkey on a 60-Hz interlaced monitor with the original sound track audible. The shutters would open and pictures of the cortex were then collected, usually at 2 Hz for 3 sec, while the stimuli were visualized by the right eye, left eye, neither eye, or both eyes. Data from 16 to 64 presentations were averaged for each stimulus condition used.

Analysis. We used the same procedure described in our earlier studies (20, 28, 29). During the course of the experiment, the sum of a center 10 × 10 patch of pixels of the charge-coupled device was averaged, enabling monitoring of the time course of the change in reflectance. Exceptionally noisy trials were rejected by using preset criteria. To obtain, for example, a map of the ocular dominance columns we took the ratio of the left eye image to the right eye image on a pixel-by-pixel basis. The resulting image was then displayed with an 8-bit frame display, using either a linear grey scale or pseudocolor scales.

RESULTS

A number of issues had to be resolved to perform optical imaging in behaving monkeys. Most of these problems did not exist in experiments on anesthetized and paralyzed animals. The first issue was whether it would be possible to measure small optical signals without immobilizing the animal with the paralytic agent previously used with anesthetized animals. Occasional movements of the awake animal might introduce motion of the cortical surface relative to the camera field of view. Since the mapping signals associated with evoked neuronal activity are often 1/1000th to 1/10,000th of the reflected light intensity without stimulation, a motion of a few micrometers might be sufficient to hamper the functional imaging. The second issue was related to the large heart beat and respiratory noise. In previous experiments on anesthetized animals, these periodic noises (often larger than the visually evoked signals) were removed by synchronizing the respiration to the heart beat and triggering the stimulus and data acquisition on the electrocardiogram (EKG). Thus, the nonvisually evoked signals were nearly eliminated by the subtraction of the two records triggered by the EKG. The third open question was whether the intrinsic optical signal useful for imaging depended on the level of anesthesia. Last, and most important, was the signal large enough to image functional architecture in the awake monkey?

Eliminating Movement Noise. We first measured the optical noise associated with voluntary body motions of the awake monkey while the head was attached to the vibration-free head holder. Head motions were not detected by careful visual inspection. Furthermore, this noise was also evaluated by more sensitive optical means; light was shined on the chamber surface and changes in the reflected intensity resulting from relative motion between the camera and the monkey's head were measured. These optical measurements indicated that the noise was smaller than 1 part in 1000 at 1 Hz. Movement noise was not detected when the monkey moved her body or arms, ate bananas, or swallowed juice. This stability can probably be attributed to the very rigid mounting of the monkey chair to the heavy vibration isolation table, without air, and to the use of rigid bars to anchor the head holder, the monkey chair, and the lens of the camera to each other, eliminating relative movements.

Time Course of Intrinsic Signals in the Awake Primate. To compare the intrinsic signals in awake and anesthetized primates we studied the time course and amplitude of the evoked intrinsic signal. The time course of the activity-dependent reflection signal was reconstructed from the 5–10 sequential frames taken during each trial. In several measurements we found that the signal in the awake monkey was slower at the optimal wavelength for imaging of 630 nm (28, 29). In the awake monkey with a stimulus duration of 2 sec, the signal continued to increase for at least 2.4 sec (Fig. 1*A*). This is in contrast to the time course in the anesthetized macaque, where the signal rapidly peaked at about 1.8 sec and then decreased towards baseline. We compared the time course observed at 630 nm in 12 imaging experiments over 6 days on the one awake monkey with 10 imaging experiments performed on multiple anesthetized monkeys and concluded that the signals in the awake animal started to decline toward baseline with a longer delay after the stimulus onset. The amplitude of the signal in the awake monkey in the example shown in Fig. 1*A* was 0.0017 (of the resting intensity of reflected light), whereas in the anesthetized animal it was only 0.0008. Although there

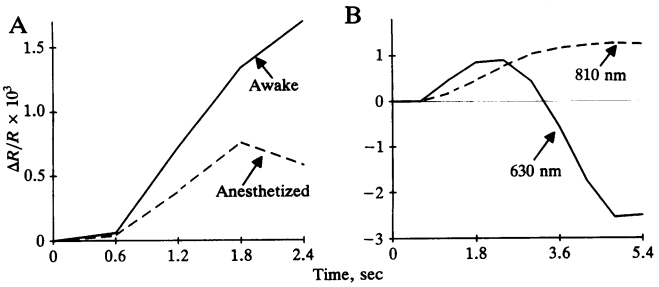

FIG. 1. Comparison of the time course and wavelength dependency of activity-dependent intrinsic signals in an awake and an anesthetized monkey. (*A*) The fractional change in the intensity of the light reflected from cortex ($\Delta R/R$) as a function of time is shown for awake and anesthetized monkeys. This time course was reconstructed from the 5 contiguous frames taken as soon as the visual stimulus was presented. Each time course represents the average of 64 responses. The stimulus was a drifting grating, of 2-sec duration, starting at time 0. Illumination wavelength was 630 nm (30-nm bandwidth). A decrease in reflection (due to an increased absorption) is plotted as a positive signal. In many experiments (see text) the downward deflection after about 2 sec was observed in anesthetized monkeys at earlier times relative to that observed for the awake monkey. (*B*) The time course of the intrinsic signal in an awake monkey at 630 and 810 nm, reconstructed from 10 frames. Same as *A*, but stimulus duration was 6 sec (see text for comparison with an anesthetized monkey).

is variability of signal size and time course in different experiments, it appears from the two sets we studied that the activity-dependent intrinsic signals were clearly *not* smaller in awake monkey (0.0015, SD 0.0006; $n = 12$) relative to those observed in anesthetized monkey (0.0009, SD 0.0005; $n = 10$) and could be on the order of 2- to 3-fold larger.

Wavelength Dependency of Intrinsic Signals in the Awake Primate. The time course of the optical signal in the anesthetized monkey is sensitive to the wavelength of light used to illuminate the cortex (20, 28). The difference in time course between infrared and visible illumination typical of the anesthetized monkey was also seen in the awake monkey. At a wavelength of 810 nm with an 8-sec stimulus, the optical signal increased monotonically (Fig. 1*B*). In contrast, at a wavelength of 630 nm and the same 8-sec stimulus, the time course of the signal was very different. The signal started to decrease after about 2.4 sec and a large undershoot was observed. These effects of wavelength were similar to those obtained in anesthetized macaques as described in our earlier reports (see figure 2 of ref. 20 and figure 3*B* of ref. 28). However, in four measurements the undershoot observed with an awake monkey was larger than that observed in three identical experiments performed on anesthetized monkeys. This study of the amplitude and the time course in the awake monkey suggested that imaging of the functional architecture should also be feasible.

Evaluation of the Respiratory Synchronization Procedure. Since it is not practical to synchronize the respiration and the data acquisition to the EKG in an awake primate, our next step was to quantify the importance of the noise reduction procedure. This evaluation was performed in two anesthetized monkeys, imaging ocular dominance and orientation column with and without the EKG synchronization procedure. Drifting gratings were used as stimuli. To reduce intraexperimental variability, the two conditions were combined in an interlaced fashion during the same imaging session. The functional maps obtained by these two procedures were of good and nearly identical quality (Fig. 2 *Middle* and *Bottom*). We examined 30 pairs of maps similar to those shown here and found that the strength of the mapping signal was the same with and without the synchronization. However, on the average the blood vessel artifacts appear to be larger by a factor of about 1.5 without the synchronization procedure (1.5, SD = 0.4; $n = 30$). This result suggested that the imaging based on intrinsic signals can be performed without the synchronization procedure. With hindsight, this finding is not surprising, because the periodic heartbeat and respiratory noise are faster than the slow intrinsic signals, and the average noise they introduced was not larger than the predominant noise source associated with the present optical imaging (namely the slow and small changes in oxygen saturation level within the microcirculation).

High-Resolution Imaging of Functional Architecture. We first attempted to image the functional architecture through the intact dura, using an illumination wavelength of 630 or 810 nm. These attempts to image the functional architecture in the awake monkey through the intact dura were not successful, even when near-infrared light (810 nm) was used. Furthermore, after the dura was thinned by removing a layer at a time using a scalpel and forceps, we were barely able to image columnar structures. These negative results were later confirmed in additional experiments on two anesthetized macaques. Clearly, near-infrared imaging (28) is easier in cats than in monkeys. We suggest that the ease of imaging through the intact dura in the cat (28) was likely due to the larger size of the cat cortex's infrared signals. The reason for this difference in optical signals in cat and monkey remains to be investigated; it could be due to the difference in packing density of cortical cells in the two species, which would affect the magnitude of light-scattering signals.

To prepare for the next series of imaging sessions, an 8 by 8 mm dural patch over the contralateral hemisphere was removed, under isoflurane and nitrous oxide anesthesia and sterile conditions. After recovery from anesthesia, the drifting gratings experiment was repeated; functional ocular dominance maps were obtained (not shown), but they were not as clear as those previously obtained in the anesthetized monkey. However, image processing was used to enhance the ocular dominance maps. It was noted during those experiments that the monkey was not particularly interested in the grating stimuli presented on the video screen. Therefore an alternative stimulus was used; the monkey viewed the video movie *Winnie the Pooh*. The same protocol used for producing ocular dominance columns images with gratings was run with the shutters alternatively covering one eye or the other in a dark room. The ocular dominance map thus obtained is shown in Fig. 3; it had a better signal-to-noise ratio than the

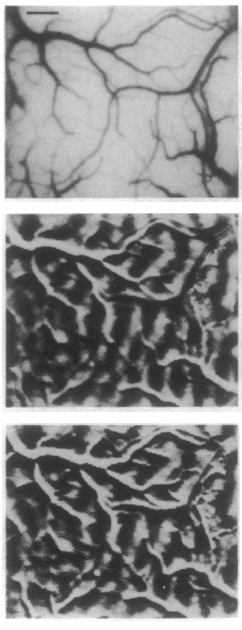

FIG. 2. Evaluation of the noise reduction procedure for functional maps. (*Top*) Cortical image. It was taken with 540-nm green light to emphasize the vascular pattern. Functional imaging was obtained with 630-nm illumination. (At this wavelength, the vascular pattern is far less visible.) (*Middle*) Ocular dominance map obtained while the artificial respiration, the data acquisition, and the stimulus presentation were always synchronized to the EKG. (*Bottom*) The same map obtained without the synchronization procedure. Note that the vascular artifacts were larger when the noise reduction procedure was not applied. To improve the statistical significance, each of these maps was obtained from 2560 frames. Functional maps obtained from fewer frames show nearly the same quality because of slow vascular artifacts in the functional maps that are not easily removed by averaging. (Scale bar = 1 mm.)

one obtained with the grating stimuli. This new, rather clear, map did confirm that the weaker ocular dominance maps obtained with the drifting gratings were indeed the correct maps. We do not presently know if the stronger map obtained with the movie indeed reflected the increased attention and interest of the monkey in this particular movie relative to the boring grating stimuli.

Histological Confirmation. To provide an independent and conclusive control for the ocular dominance maps, we decided to immediately compare the cytochrome oxidase histology from this cortical region to the optically imaged blobs. Fig. 4 *Upper Left* shows the OD optical map; the blobs were revealed by marking the regions of the highest monocular responses for each eye (29). To demonstrate this, a pseudocolor map was used where regions of extreme monocularity are shown in blue and other cortical regions appear red or green depending on whether they belong to the right or the left ocular dominance columns (Fig. 4 *Upper Right*). A gray level map in which only highly monocular regions appear dark is shown in Fig. 4 *Lower Right*. The histologically determined blobs (24) are shown in Fig. 4 *Lower Left*. Considering the possible distortion of the histological sections, the correspondence between the location of the optically determined blobs and the histologically determined blobs is good. This histological confirmation provides evidence for the validity of the optical maps.

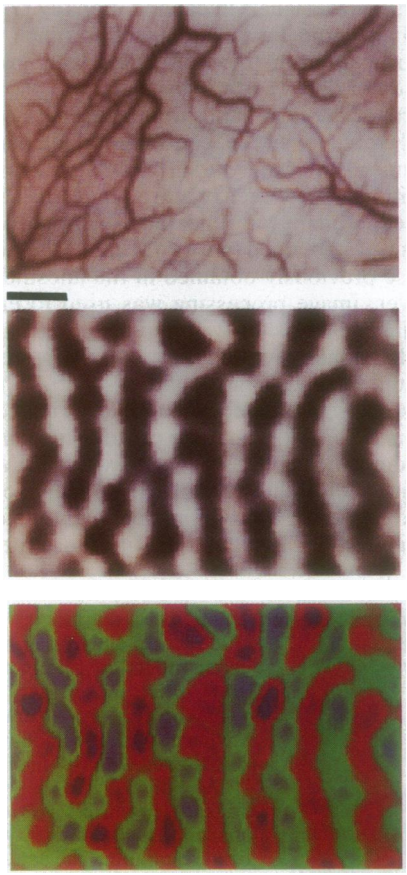

FIG. 3. Imaging of ocular dominance columns in the awake monkey obtained by monocular presentation of a video movie. (*Top*) Picture of the imaged area taken in green light. (Scale bar = 1 mm.) (*Middle*) Ocular dominance map. This map was obtained by dividing 48 cortical images taken when the right eye was viewing the video movie *Winnie the Pooh* by 48 cortical images taken when the left eye viewed the movie. Note, however, that these best frames were selected post hoc from 640 frames collected for each eye. (*Bottom*) Same data as *Middle*, except that a pseudocolor map was used. The intensity of the red denotes the dominance by the left eye and intensity of the green denotes the dominance by the right eye. The blue regions correspond to the center of the highest monocular activity and lie in the center of each ocular dominance column.

DISCUSSION

This report indicates that it is possible to use optical imaging techniques for the exploration of functional architecture in awake primates. The combined advantages of optical imaging and the awake behaving primate are likely to contribute to the elucidation of functional maps related to higher cognitive functions in several cortical areas *in vivo*. The fundamental benefit of this approach will be that many *in vivo* functional maps can be obtained from the same patch of cortex, as a function of multiple stimuli used, or the skills acquired, in a way not previously possible.

It was interesting to find out that, in general, the intrinsic signals in the awake monkey were similar to those obtained in anesthetized monkeys. This result should be contrasted with PET imaging, in which functional imaging can be obtained in awake patients but not in anesthetized patients. Although the interaction of neuronal activity with the microcirculation underlies both imaging techniques, the different effects of anesthesia are not necessarily surprising. PET imaging is mostly sensitive to changes in blood flow, while optical imaging is mostly sensitive to changes in blood oxygenation level, blood volume, and light-scattering changes (28). The qualitative differences observed for the microcirculation responses in awake monkeys need further quantitative examination; the finding that the deflection of optical signal (Fig. 1*A*) was delayed suggests that activity-dependent changes in oxidation in the awake animal are slower than in the anesthetized animal. The increased undershoot at 630 nm (Fig. 1*B*) suggests that changes in blood flow are faster in awake than in anesthetized animals (28).

The result that the OD map obtained for the awake monkey (Figs. 3 and 4) is significantly better than those obtained for anesthetized monkeys (Fig. 2) warrants brief discussion. This improvement was obtained by our selection of 48 frames for each eye out of a total of 1280 frames to optimize the OD map. The selection process was based on inspection of the ocular dominance map obtained by dividing each frame by the average of all frames. Since the noise level is reduced considerably when all frames are averaged, it was possible to select the individual frames in which the blood vessel artifacts were small and the ocular dominance map was visible. The total exposure time for the selected frames was thus only approximately 60 sec. Similar optimization procedures in anesthetized monkey studies should also result in improved maps.

The present imaging protocol can be improved in many ways. First, if all the acquired frames are stored, then the *post hoc* selection procedure can be improved. (Here, every 16 stimulus presentations were averaged.) Second, the stimulus duration and intertrial interval can be optimized by extensive experimentation as previously done for the anesthetized monkey. Since the signals were somewhat slower it appears that a longer delay and duration for frame acquisition may improve the quality of functional maps in the awake monkey. Third, recent technical improvements in optics and data collection (30) are likely to shorten the duration of the measurements dramatically. Fourth, the monkey can be trained to fixate on the center of the screen. This will ensure that the monkey attends to the stimulus and the retinal locus of the stimulus can be controlled. Finally, additional work is required to determine how to maintain a primate with a resected dura for an extended period of time, as it was not possible to image the functional architecture through the intact dura. One possibility is to implant a transparent artificial dura.

The present study suggests that the optical imaging technique is a useful tool to study cortical development, plasticity, or recovery of function after injury or lesions, or as a

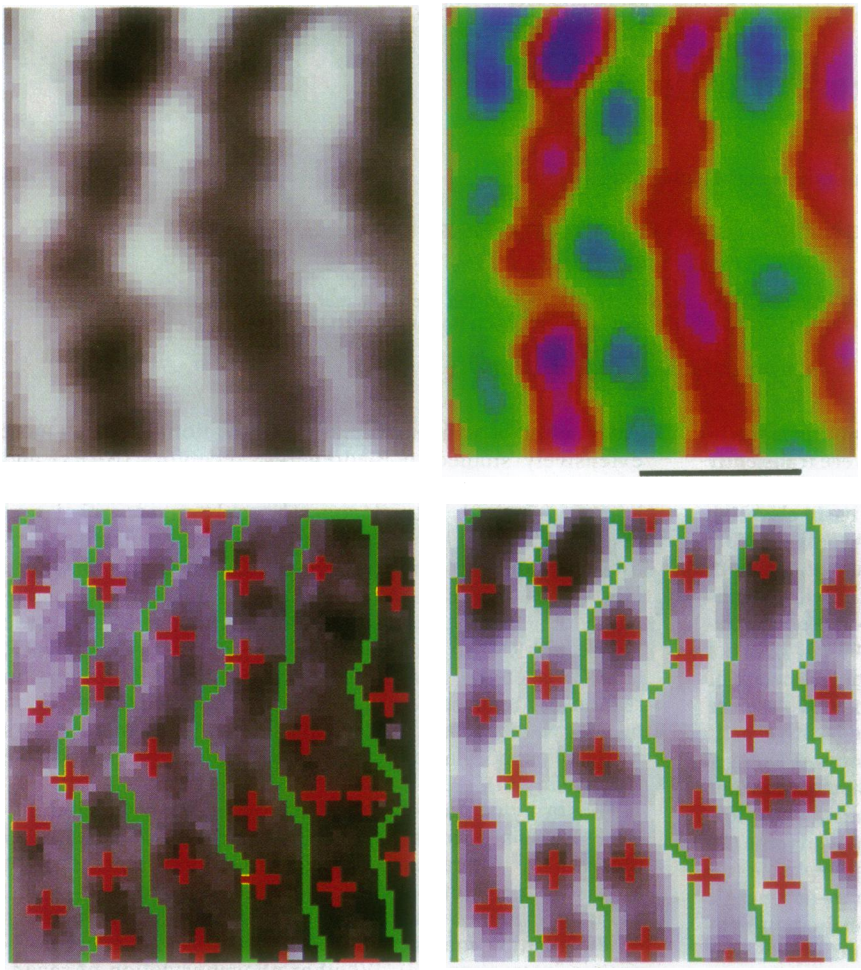

FIG. 4. Histological confirmation of the optical map. (*Upper Left*) Enlarged image of a portion of the OD map (taken from the bottom left of the map). (*Upper Right*) Same map, using the pseudocolor scale. (*Lower Right*) Same map with the centers of extreme monocularity coded in gray scale and manually marked by small red crosses. (*Lower Left*) Postmortem cytochrome oxidase histology of the same cortical region. The pattern of red crosses was transferred from the optical image of the monocularity centers, showing their clear correspondence to most of the cytochrome oxidase blobs. The two small crosses indicate areas of poor correspondence between the optical and histological blobs. (Scale bar = 1 mm.)

result of transplantation. Similarly, the use of awake primates and optical imaging can contribute to the study of the function of primary sensory area as well as greatly assisting *in vivo* studies of higher brain functions such as motion and color processing, attention, motivation, memory, and learning.

The spatial resolution of functional maps in the awake primate brain indicates that this approach may be particularly useful as a mapping tool in human neurosurgery. Optical imaging should allow the intraoperative evaluation of epileptic foci. In patients undergoing microsurgical removal of tumors, or during neurosurgical treatment of vascular and neoplasmic lesions, it should also be possible to precisely map functional borders on the cortical surface during the surgical procedure. In addition to providing the neurosurgeon with clear reference points to guide the resection, in the future microsurgical approaches can be applied to minimize damage to essential cortical tissue. Clinical neurological evaluations might benefit from this technique by directly visualizing cortical processing in human patients.

We thank Drs. T. N. Wiesel, T. Bonhoeffer, L. C. Katz, C. D. Gilbert, and D. Ts'o for their constructive comments and useful suggestions and Dan Ts'o, Eugene Ratzlaff, and Kaare Christian for their support with programming and electronics and Mr. Shlomo Artzi for his valuable technical assistance. This work was supported by IBM and National Institutes of Health Grant NS 14716 to A.G.; R.M.S. was supported by the Charles H. Revson Foundation.

1. Evarts, E. V. (1971) *Int. J. Neurol.* **8**, 321–326.
2. Kojimas, S. & Goldman-Rakic, P. S. (1984) *Brain Res.* **291**, 229–240.
3. Mountcastle, V. B., Andersen, R. A. & Motter, B. C. (1981) *J. Neurosci.* **1**, 1218–1225.
4. Perrett, D. I., Smith, P. A. J., Potter, D. D., Mistlin, A. J., Head, A. S., Milner, A. D. & Jeeves, M. A. (1985) *Proc. R. Soc. London Ser. B* **223**, 292–317.
5. Richmond, B. J., Wurtz, R. H. & Sato, T. (1983) *J. Neurophysiol.* **50**, 1415–1432.
6. Schlag, J. & Schlag-Rey, M. (1985) *Exp. Brain Res.* **58**, 208–211.
7. Fuster, J. M. & Jervey, J. P. (1982) *J. Neurosci.* **2**, 361–375.
8. Wise, S. P. & Mauritz, K. H. (1985) *Proc. R. Soc. London Ser. B* **223**, 331–354.
9. Moran, J. & Desimone, R. (1985) *Science* **229**, 782–784.
10. Goldberg, M. E., Bushnell, M. C. & Bruce, C. J. (1986) *Exp. Brain Res.* **61**, 579–584.
11. Harwerth, R. S., Smith, E. L., Boltz, R. L., Crawford, M. L. J. & von Noorden, G. K. (1983) *Vision Res.* **23**, 1501–1510.
12. Merzenich, M. M., Kaas, J. H., Wall, J. T., Nelson, R. J., Sur, M. & Felleman, D. J. (1983) *Neuroscience* **8**, 33–55.
13. Jenkins, W. M., Merzenich, M. M., Ochs, M. T., Allard, T. & Guic-Robles, E. (1990) *J. Neurophysiol.* **63**, 82–104.
14. Lisberger, S. G. (1984) *Science* **225**, 74–76.
15. Murray, E. A. & Mishkin, M. (1986) *J. Neurosci.* **6**, 1991–2003.
16. Newsome, W. T. & Pare, E. B. (1988) *J. Neurosci.* **8**, 2201–2211.
17. Schroeder, C. E., Tenke, C. E., Givre, S. J., Arezzo, J. C. & Vaughan, H. G., Jr. (1990) *Brain Res.* **515**, 326–330.
18. Steinschneider, M., Arezzo, J. C. & Vaughan, H. G., Jr. (1990) *Brain Res.* **519**, 158–168.
19. Skarda, C. A. & Freeman, W. J. (1987) *Behav. Brain Sci.* **10**, 161–173.
20. Grinvald, A., Lieke, E., Frostig, R. D., Gilbert, C. D. & Wiesel, T. N. (1986) *Nature (London)* **324**, 361–364.
21. Salzberg, B. M., Davila, H. V. & Cohen, L. B. (1973) *Nature (London)* **246**, 508–509.
22. Grinvald, A., Frostig, R. D., Lieke, E. & Hildesheim, R. (1988) *Physiol. Rev.* **68**, 1285–1366.
23. Hubel, D. H. & Wiesel, T. N. (1977) *Proc. R. Soc. London Ser. B* **198**, 1–59.
24. Wong-Riley, M. & Carroll, E. W. (1984) *Nature (London)* **307**, 262–264.
25. Hendrickson, A. E. (1985) *Trends Neurosci.* **8**, 406–410.
26. Livingstone, M. S. & Hubel, D. H. (1984) *J. Neurosci.* **4**, 309–356.
27. Perlmutter, J. S., Lich, L. L., Margenau, W. & Buchholz, S. (1991) *J. Cereb. Blood Flow Metab.* **11**, 229–235.
28. Frostig, R. D., Lieke, E. E., Ts'o, D. Y. & Grinvald, A. (1990) *Proc. Natl. Acad. Sci. USA* **87**, 6082–6086.
29. Ts'o, D. Y., Frostig, R. D., Lieke, E. & Grinvald, A. (1990) *Science* **249**, 417–420.
30. Ratzlaff, H. E. & Grinvald, A. (1991) *J. Neurosci. Methods* **36**, 127–137.